CHAPTER II

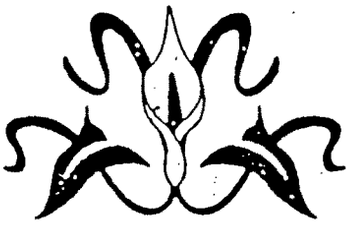

CHAPTER II

PREPARATION AND CHARACTERIZATION OF PYROCHRORES

2.1 INTRODUCTION

Most of the properties like electrical and magnetic properties of pyrochlores predominantly depend on their densification, porosity and microstructure, which in turn depend on the method of preparation and thermal history of the materials. Purity of starting materials, mixing, sintering temperature and time. Partial pressure of oxygen inside the furnace, rate of cooling and all other related factors considerably affect the properties of the final product. Also microstructural factors such as grain size, defect concentration, inclusions, pores, grain shape and prefered orientation etc, sensitively influence the properties of ceramic material.

This chapter covers the method of preparation of pyrochlores and the X-ray diffraction studies undertaken to findout the formation of pyrochlore as charecterized by the spinel structure and its characteristic diffraction pattern and to study the variation of lattice parameter with composition in mixed pyrochlore systems under study.

2.2 PREPARATION OF PYROCHLORES

In the present study the method used for the preparation of pyrochlores is ceramic method or oxide method.

There are four steps in the preparation of pyrochlores by ceramic method.

a) To form intimate mixture of starting oxides

b) Presintering or calcination

c) Milling and pressing in desired shape

d) Sintering

2.2.1 CERAMIC METHOD.

In this preparation, the starting materials are allowd to undergo solid state reaction and therefore it is usually called ceramic process. High purity AR grade oxide materials are mixed together in the proportions required in the final product. This mixing is best performed by wet milling for sufficiently long period of time in a rubber lined pot using stainless steel balls. The attritor and vibratory ball mil are ususally used with an advantage to cut down mixing times which with a rotatory ball mill may lost for serveal hours. After milling the mixture is dried. The flow chart for ceramic method shown in fig. 2.1

2.2.2. PRESINTERING

The dry mixture is presintered at a suitable temperature which is lower than the final sintering temperature.

According to Swallow and Jordan (1) the purpose of presintering or calcination is four fold.

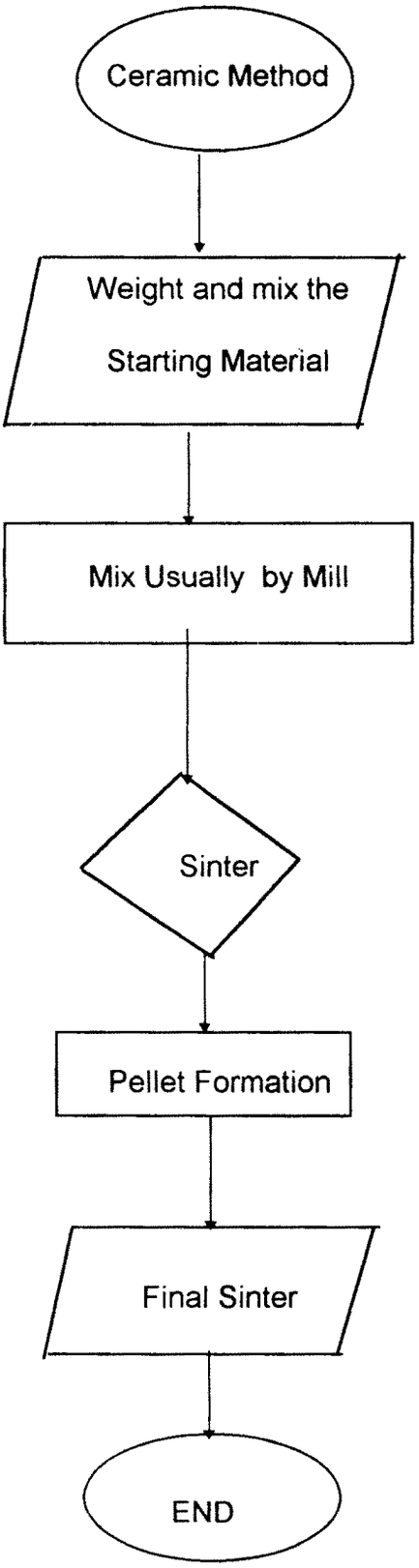

Fig. 2.1 Ceramic Method.

I) To decompose carbonates and higher oxides and give out a first installment of evolution of gas, reducing thereby the final installment at the time of final sintering

ii) To homogenize the final materials

iii) To reduce the effect of variations in compositions of raw materials.

iv) To reduce or control the shrinkage which occurs at the time of final sintering

From the above it is clear that in the stage of presintering, the solid state reaction in not the aim. However at temperatures that are usually employed for presintering or calaination, the diffusivity of ions is sufficient to cause solid state reaction to a small extent. The amount of reaction depends on the reactivity of the components and the presintering temperature (2)

2.2.3. MILLING AFTER PRESINTERING

Milling of powder involves reactivity as the small particles size is achieved. The milled powder is then used for preparing the final product of the rquired shape.

2.2.4. FINAL SINTERING

The uniform grainsize of pyrochlore with intragrannular pores and discontinuous graingrowth is achieved during the final sintering Besides this it also increases the density of the pyrochlores. Final sintering is the most common process of integrating and preparing solid state materials . As the final major step in the preparation of pyrochlores the sintering must fulfil three requirements, namely

I) to bond the particles together so as to impart sufficient strength to the products

ii) to densify the grain compacts by eliminating the pores, and

iii) to homogenize the materials by completing the reactions left unfinished in the presintering step. As far as their mechanism is concerned the first two requirements are closely related. The equation for the initial stage of the sintering process is given by

$$\frac{\Delta L}{L} = \left[\frac{(Ad\Upsilon' \Omega)\, t}{(3\bar{\Upsilon} KT)}\right] 1/2 \qquad \text{----------(2.1)}$$

where, ΔL is the shrinkage of the compact

Ω is the volume of single vacancy

D is the coefficient of self diffusion for the slowest moving species

Υ' is the surface energy

$\bar{\Upsilon}$ is the arerage radius of the particles

t is the sintering time

and A is the constant of approximate value of unity

Equation (2.1) indicates that the sintering fulfils requirements i) and ii) more efficiently when the compact features have high surface energy and self diffusivity and fine particles

We assume that the cations are present in correct proportions, but they are affected by the time and temperature of sintering the partial pressure of oxygen or any other sintering atmosphere and cooling rate. During sintering densitication and graingrowth occur at the same time to lead varity of microstructures.

Volume diffusion is the main transport mechanism in an ionic solid, such as spinels, Nabarrow (3), Herring (4) theory for diffusional microcreep is considered to be main mechanism for densification. The surface of the pores acts as source of vacancies. Migration of vacancies occurs as a result of concentration gradient between the curved surfaces of the pores and equilibrium vacancy concentration under the flat surface (C_o). The vacancy concentration (C_r) under the surface of radius of curvature (r) is given by kelvins equation.

$$C_r = C_o \exp \frac{(2r_s a^3)}{(r.KT)} \qquad \text{----------(2.2)}$$

where r_s is surface tension, a^3 is the vacancy volume.

As the concentration of grainboundary is equal to (C_o), vacancy migrates at a temperature, where the mobility is sufficiently high from the pore surface to the grain boundaries. In grain growth the grainboundary energy is decreased. When the boundaries move to their centre of curvatue; the rate of grain growth (5) is given by

$$D - Do = Kt^n \qquad \text{----------(2.3)}$$

Where Do is the particle size

K is the temperature dependant factor and

t is the time

The expected rate of graingrowth is proportional to $t^{1/2}$. However in practice it is proportional to $t^{1/2}$, due to the presence of impurities and inclusions in the grain boundaries. Zener (6) has given a purely empirical relationship for discontinuous graingrowth,

$$Dc_r = \frac{di}{fi} \qquad \text{----------(2.4)}$$

where, di is the diameter of inclusion and fi is the fraction volume

The continuous graingrowth may lead to a deplex structure of gaint grains in a matrirx of small grains. This appears to be quite common in technical ceramics leading to a characteristically porous structure. It is because rapid growth entraps pores in the grains which is scarcely possible to eliminate due to their great distance from the grain boundaries.

In order to maintain exact proportions of metal ions in the final product, careful control of sintering atmosphere is very important.

2.3 GRAIN GROWTH

The source of driving the graingrowth is the grain boundary. As the grainsize increases the energy of boundary decreases and the boundaries move towords the centre of curvature. The presence of impurities in the grainboundaries hinders the graingrowth. The graingrowth occurs until the ratio of diameter of inclusions to the volume fraction is equal to the critical diameter of grains when pores or inclusions disappear during heating the large grains are formed. The exaggerated graingrowth ocaurs when average grainsize reaches the critical size.

2.4 POROSITY:

Porosity is a phase which is always present in ceramic processing of powder compacts . To obtain low porosity, it is useful to promote the sintering rate by using powders with large surface area. Larger pores will grow at the expense of small pores in it's direct vicinity by volume or grainboundary diffusion of vacancies. However small pores move along with moving grainboundary due to vacancy gradient over the two pore surfaces. It has been found that at low rate of sintering, the pore growth becomes predominant and if it is discontinuous graingrowth is observed.

The microstructure with larger pores is related to compounds having low sintering rate is achieved when the condition,

$$D_c C_c = D_o C_o$$ is satisfied

where, D_c is the diffusion constant of cation vacancies.

D_c is the diffusion constant of oxygen vacancies.

C_c is the bulk concentration of cation vacancies.

and C_o is the bulk concentration of oxygen vacancies.

2.5 ACTUAL METHOD OF PREPARATION OF PYROCHLORE SAMPLES :

In the present study, the samples were prepared by standard ceramic method using AR grade oxides. The oxides of rare earths are weighed according to required mole proportions on a semimicrobalance having least count of 0.001 gm. The gram molecular weights of these oxides are

$Y_2 O_3$ = 225.8082 gm mole

$Ce_2 O_3$ = 328.2382 gm mole

$Sm_2 O_3$ = 348 .7182 gm mole

Also the oxides of Titanium and Tin were weighed in same way, so as to mix with rare earth oxides.

2 Tio_2 = 159.7976 gm mole

2 SnO_2 = 301.3776 gm mole

$$\therefore A_2^{(3+)}O_3 + 2\ B^{(4+)}O_2 \longrightarrow A_2^{(3+)}\ B_2^{(4+)}O_7$$

The oxides of Titanium and Tin were mixed thoroughly with each rare earth oxide in an agate morter with acetone. The mechanical mixing was carriedout in acetone medium carefully without any loss of powder and mixture was dried in an oven at a temperature of about 100 ^{0} C The dry mixtures were then transferred into platinum crucibles and were presintered at 700^0 C for 7 hours in air by using a globar furnace A chromel alumel thermocouple was used for the measurement of temperature of the furnace. The samples were allowed to cool to room temperature slowly at the rate of 80^0 C per hour. The presintered powder was then ground in agate- morter in acetone medium for two hours and finally powder was collected in a clean glass tube.

2.6.1 PELLET FORMATION :-

About two grams of presintered dry powder was taken in an agate morter and milled to have fine particles. This dry powder was then transferred into a die having 1.5 cm diameter and pressed in a hydraulic press with the pressure of the order of 8 to 10 tonnes per square inch about 5

minutes. After removing the load, pellet was taken out from the die, several pellets of different compositions were prepared using the same technique.

2.6.2 FINAL SINTERING

The pellets thus prepared were placed on platinum foil in a globar furnace at a temperature of 1150^0 C about 24 hours in an air medium for the completion of solid state reaction. Then the furnace was cooled at the rate of 80^0 C/ hr.

For X-ray diffraction studies the pellets were again ground in a ball mill and the powder that was obtained was seived through a mesh of 10 microns in order to obtain uniform grain size of the product. Some pellets were kept in reserved for their use in determination of electrical properties.

2.7 X-RAY DIFFRACTOMETER

X-ray diffraction is a tool for the investigation of the fine structure of matter. This technique is the outcome of Van Laue's discovery in 1912. According to Laue, crystals diffracts X-rays. The diffraction pattern reveals the structure of crystal. At first X-ray diffraction was used only for the determination of crystal structure. Later on other uses were developed. Today the method is applied not only for structure determination but also for solving diverse problems related to chemical analysis, measurement of particle size and for the determination of the orientation of the crystals. X-rays are effectively used for diffraction as, X-rays have the wavelength comparable to the lattice parameter of the crystal.

2.7.1 PRINCIPLE OF DIFFRACTOMETER

The principle of X-ray diffractometer and main features are shown in Fig 2.2 The incident beam of X-rays is allowed to pass throuth the slit 'A' of the Collimator. As the crystallites are randomly oriented, a reflection of particular position is due to set of atomic planes which satisfy

$$2 d \sin \varphi = n\lambda$$

where N = Order of diffraction.

λ = Wavelengh of X-rays.

φ = is the glancing angle

d = is the interplener distance.

The diffracted beam gets converged and focussed at a slit 'F' which further enters the counter 'G' with the help of special slit 'B' The difracted beam is then collimated. The counter G is connected to a count rate meter and output of the circuit is fed to a fast automatic recorder. It records counts per sec. Versus '2φ' for corresponding Bragg reflection. Hoverer in modern X-ray diffractometer proportional or scintillation counter is mounted which records automatically a graph of intensity of X-rays with respect to Bragg angle.

The main advantage of the diffractometer over the Debye - scherrer powder method is it gives a quantitative measure of intensity.

The location of the centroid of the recorded peak give $2\varphi_{hkl}$ for corresponding Bragg's condition. The reciprocal lathice lies on to surface of radiclels (hkl)

Schematic X-ray Diffractometer

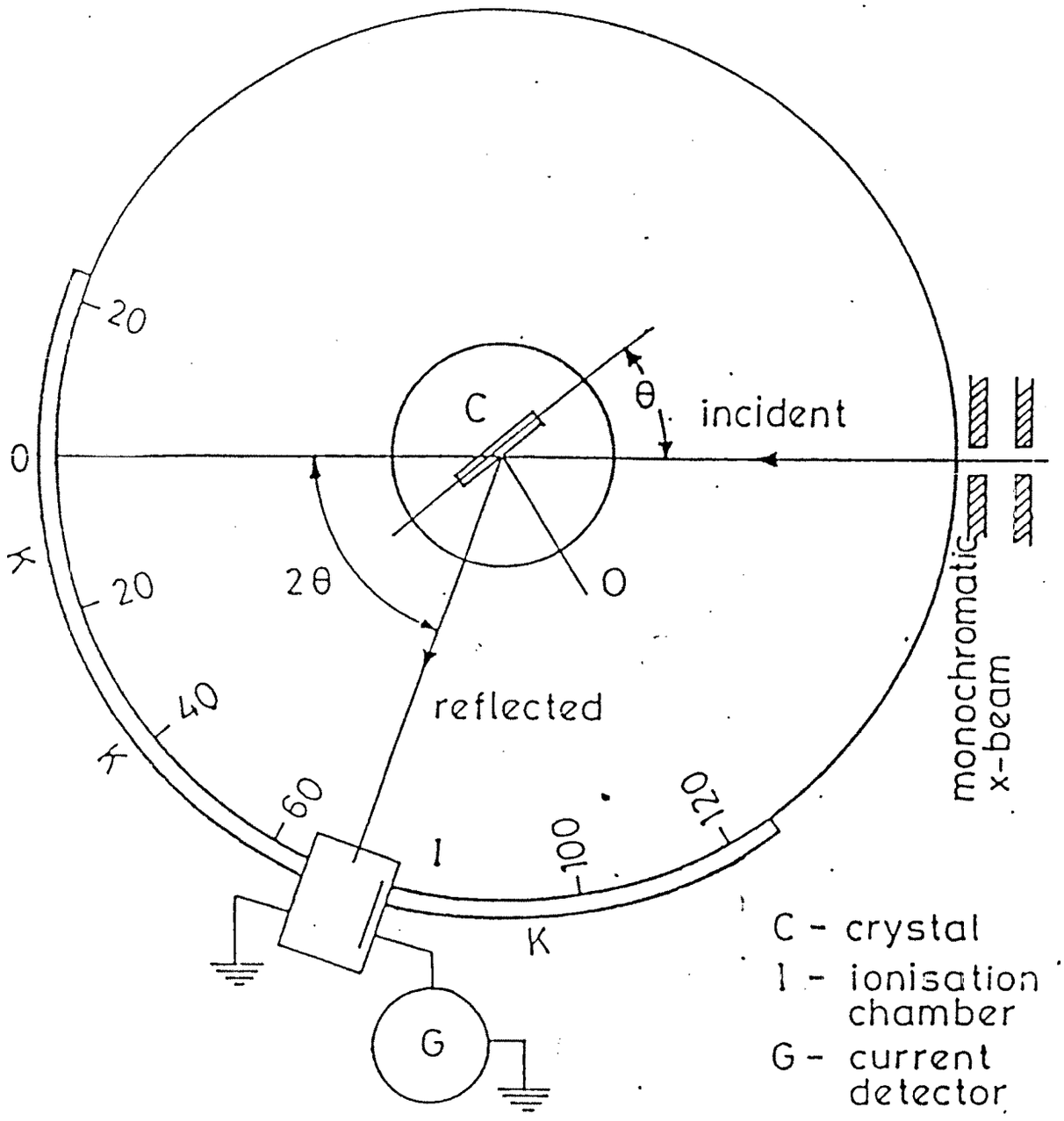

Fig. 2.2

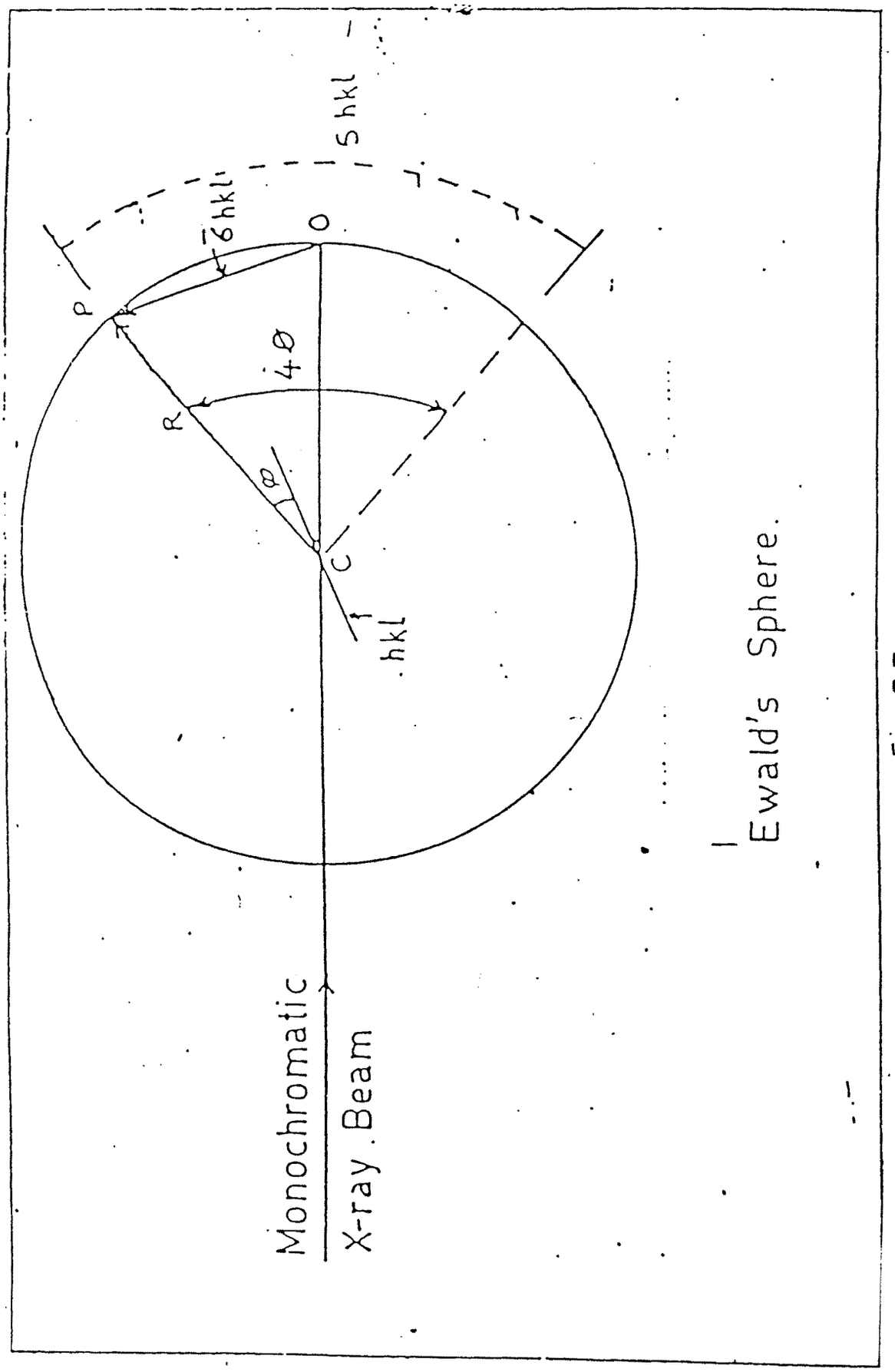
Monochromatic
X-ray Beam
Ewald's Sphere.
hkl
C
R
2θ
θ
P
O
S hkl
S̄ hkl

Fig. 2.3

and is oriented by every possible value of hkl cutting the Estwald's sphere as shown in fig (2.3). By geometry of Estwald's

$$4\varphi_{hkl} = S_{hkl}/R$$

2.7.2 EXPERIMENTAL

For present investigation the powder samples were scanned for X-ray diffraction on Philips make computerised X-ray diffractometer PW 1710 using Cukα radiation, available in CFC, shivaji university kolhapur. The diffraction angle varied between 20^0 to 80^0

By considering the predominant peak on the pattern the lathice parameters were determined for different samples. The planes (h,k,l) and correlated 'a' value thus obtained were used to calculate 'd' values which were then compared to observed 'd' values given directly by Bragg law. The experimental interplaner spacings can be indexed as a face centered cubic cell. Peak intensities and the systematic absences were typical of the pyrochlere structure.

2..8 RESULTS AND DISCUSSION

The complete X-ray analysis involves charecrization and structure determination. The standard pyrochlore structure having Fd3m space group gives rise to diffraction peaks with particular specific indices. If the compound exhibits the occurance of these peaks then, we may confirm the formation of pyrochlore lattice. In the present system, typical lines pertaining to cubic pyrochlore structure do appear and this confirms the formation of pyrochlore compound. The standard spinel lathice of pyrochlore possesses

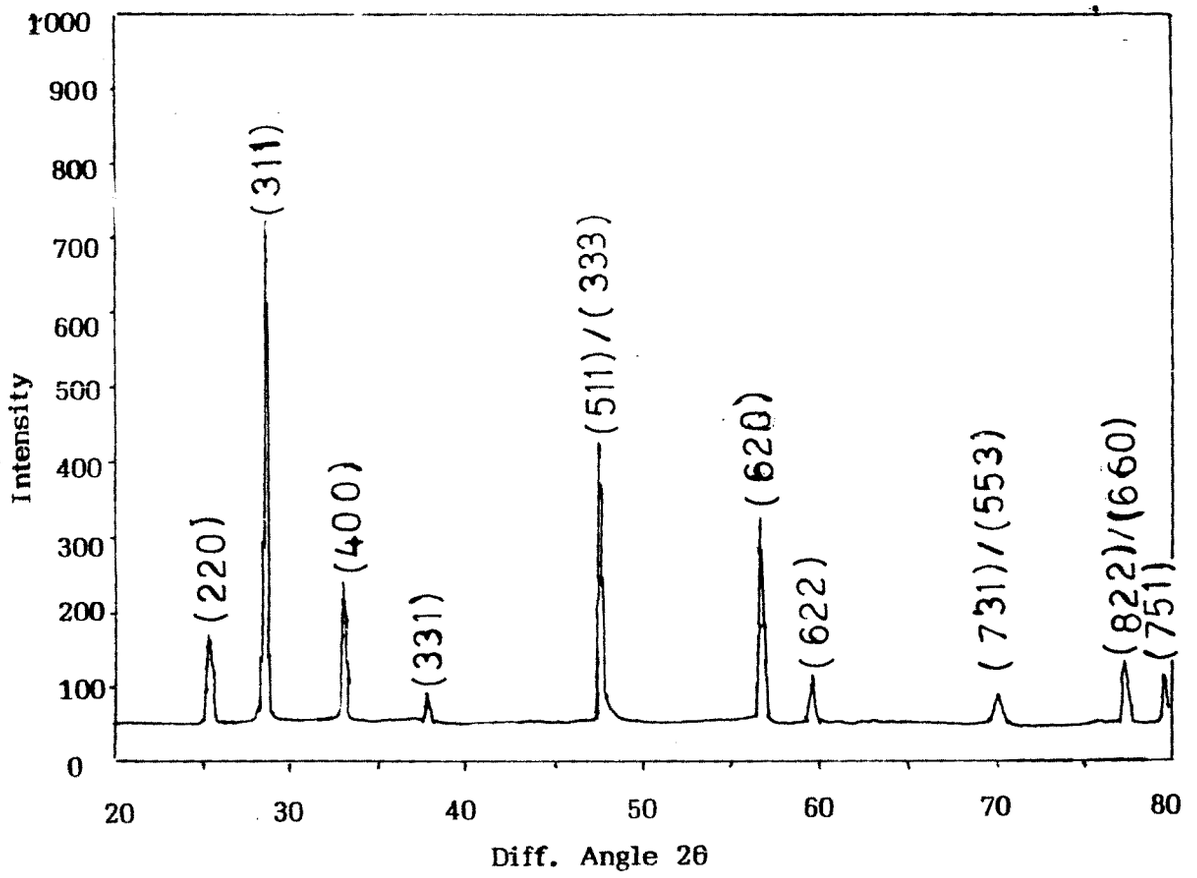

Fig. No.2.4 : X-ray diffraction pattern for the sample $Ce_2Ti_2O_7$

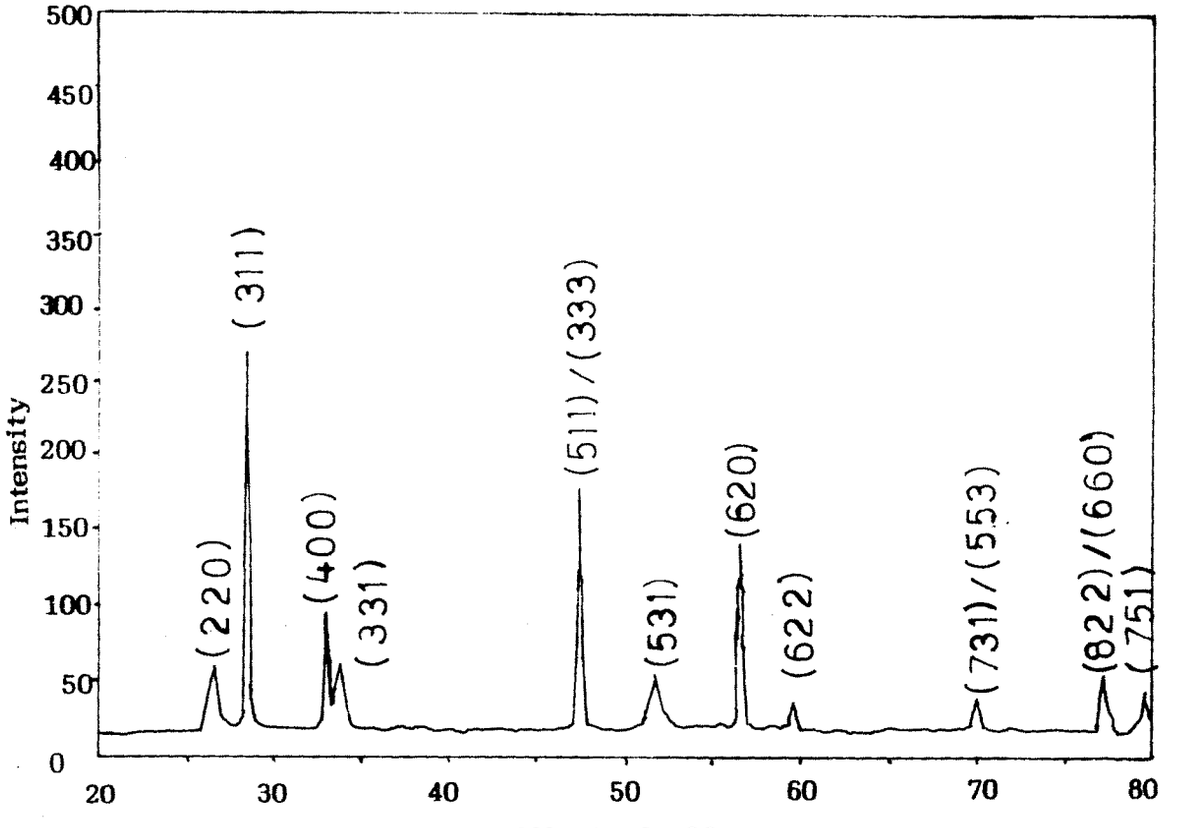

Fig. No. 2.5 : X-ray diffraction pattern for the sample $Ce_2Sn_2O_7$

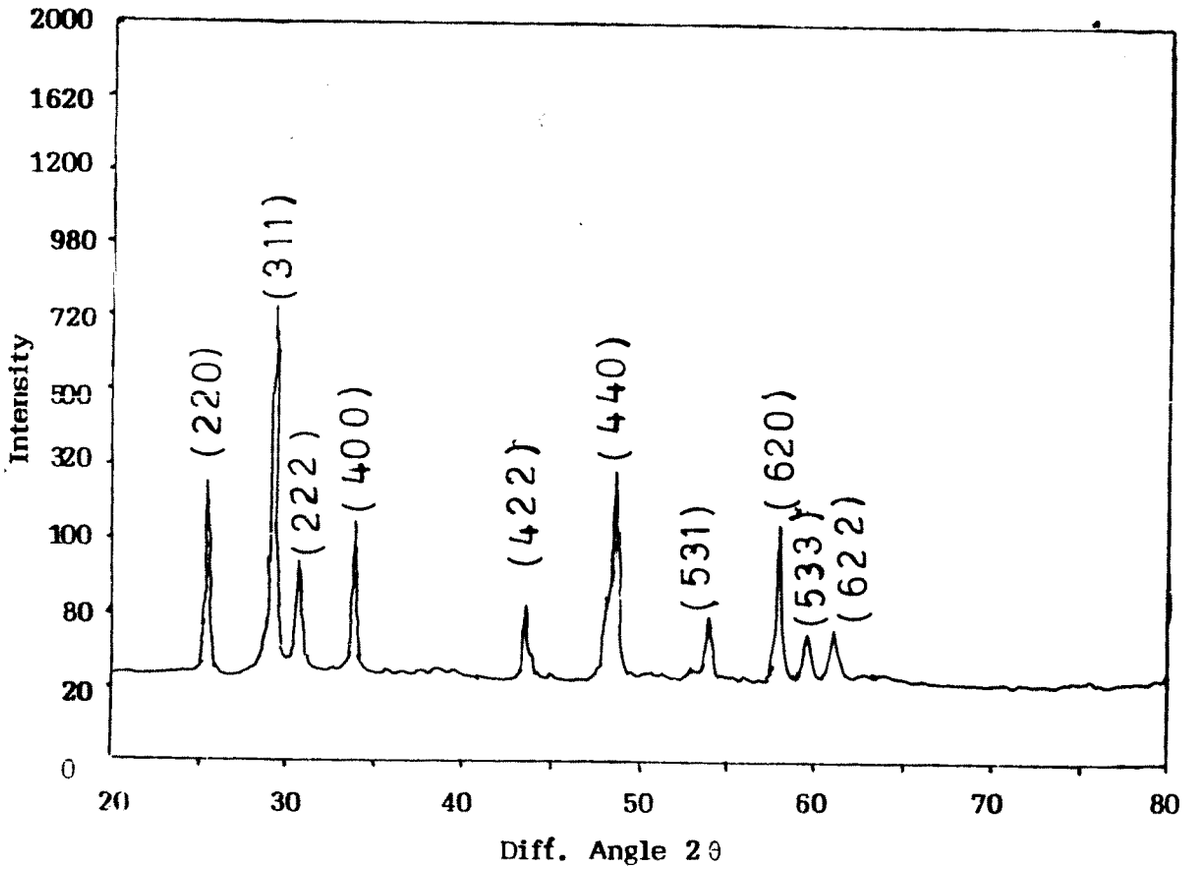

Fig. No. 2.6 : X-ray diffraction pattern for the sample $Y_2Ti_2O_7$

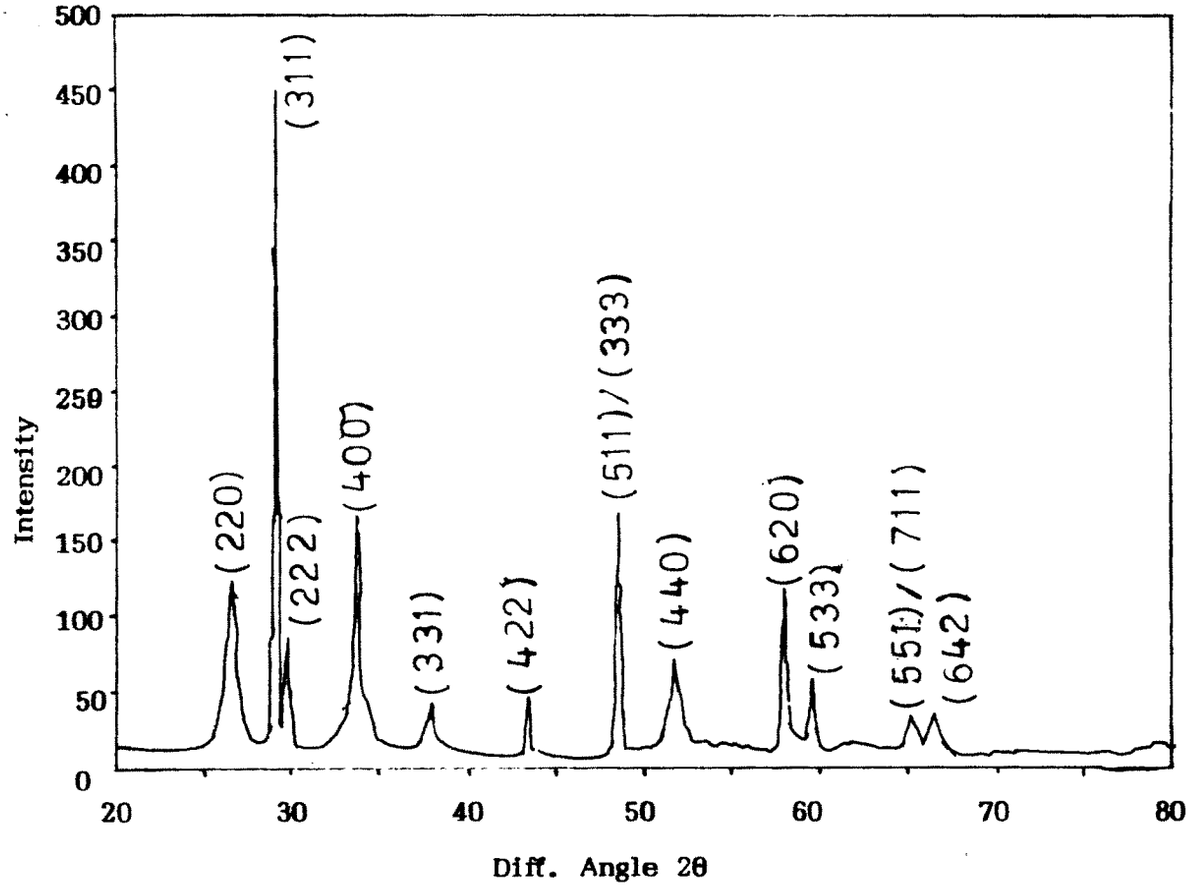

Fig. No.2.7 : X-ray difraction pattern of the sample $Y_2Sn_2O_7$

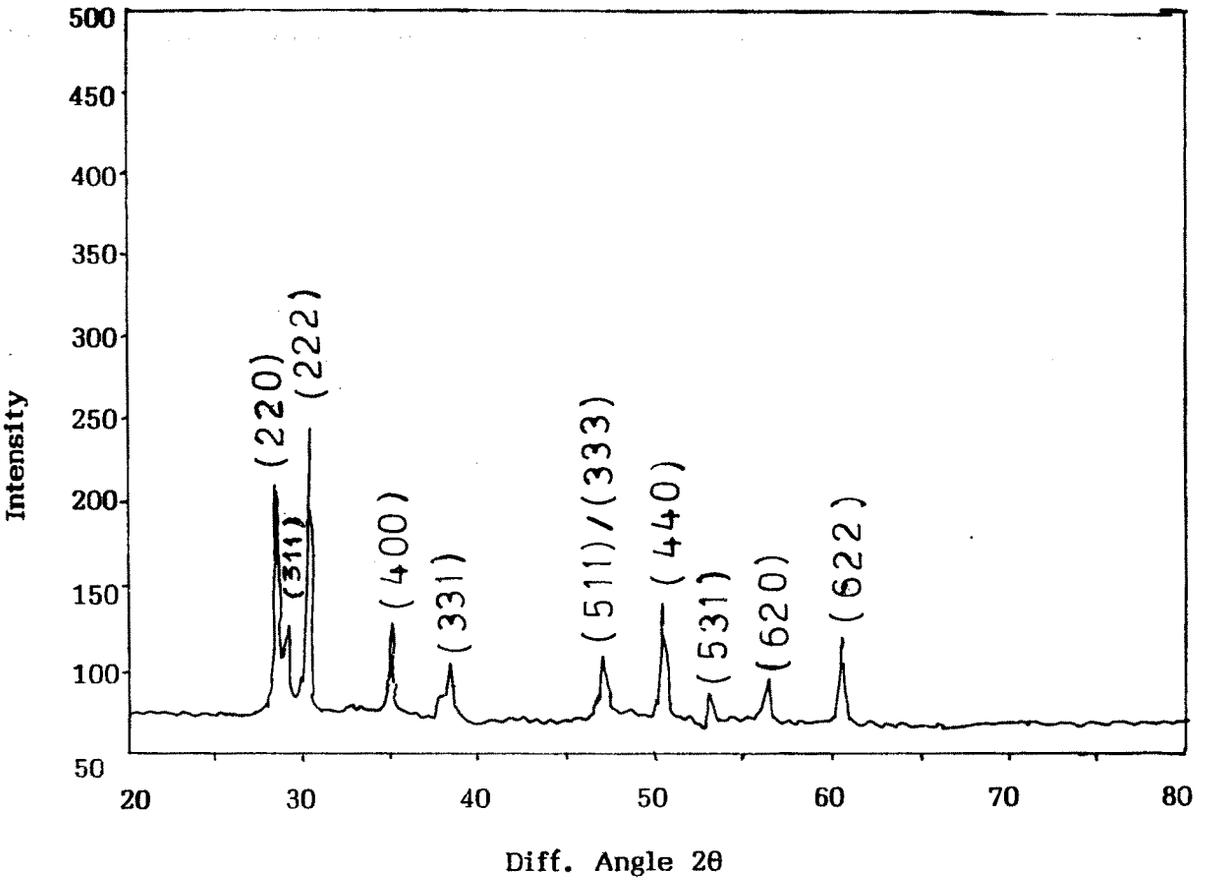

Fig. No. 2.8 : X-ray diffraction pattern of the sample $Sm_2Ti_2O_7$

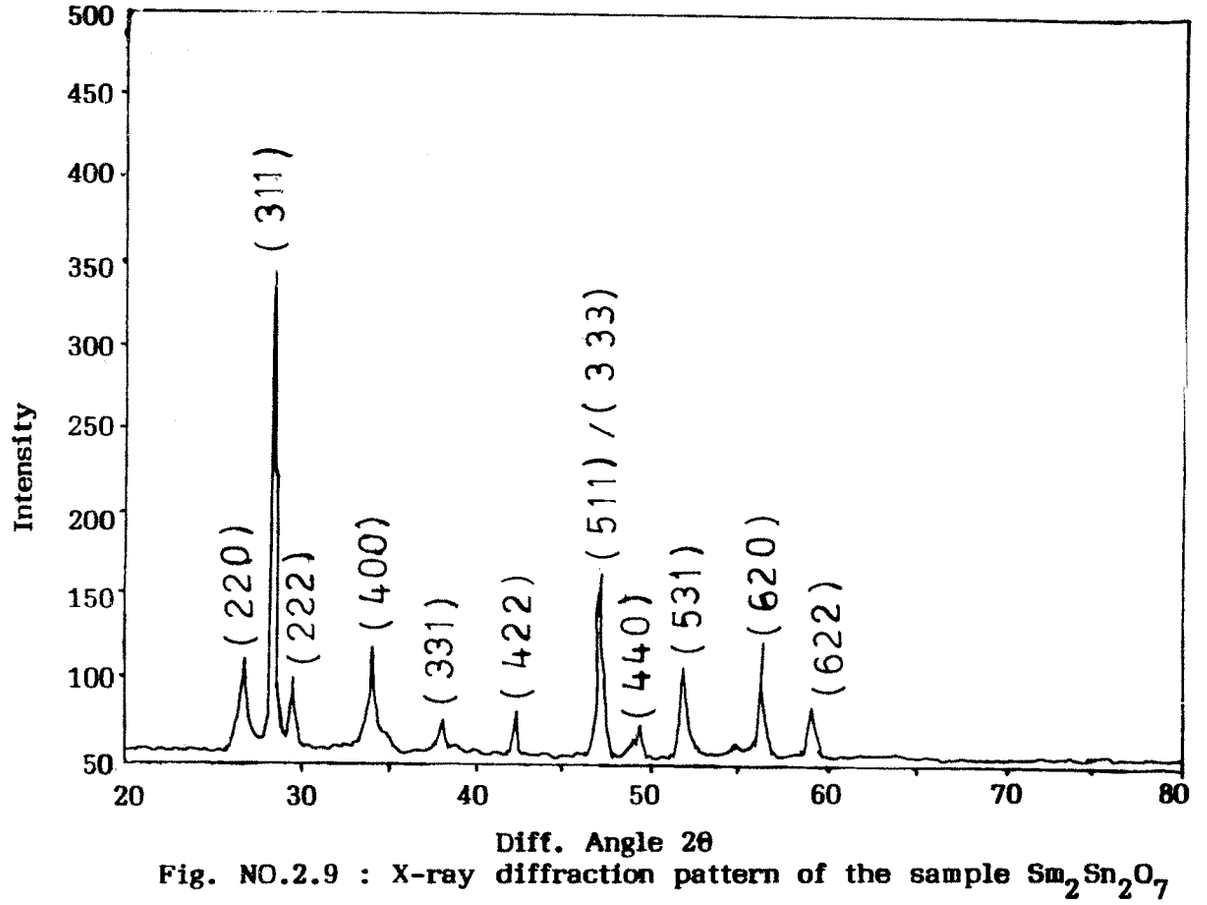

Fig. NO.2.9 : X-ray diffraction pattern of the sample $Sm_2Sn_2O_7$

Table 2.1 MILLER INDICES AND hkl PLANES FOR $Ce_2Ti_2O_7$

Plane hkl	dobs Å	dcal Å
220	3.64	3.65
311	3.11	3.11
400	2.58	2.58
331	2.37	2.36
511/333	1.91	1.98
620	1.62	1.63
622	1.55	1.55
731/553	1.34	1.34
822/660	1.21	1.21
751/555	1.19	1.19

Table 2.2 MILLER INDICES AND hkl PLANES FOR $Ce_2Sn_2O_7$

Plane hkl	dobs Å	dcal Å
220	3.66	3.66
311	3.12	3.12
400	2.64	2.64`
331	2.36	2.38
511/333	1.95	1.99
531	1.75	1.75
620	1.64	1.64
622	1.55	1.56
731/553	1.34	1.35
822/660	1.22	1.22
751/555	1.19	1.19

Table 2.3 MILLER INDICES AND hkl PLANES FOR $Y_2Ti_2O_7$

Plane hkl	dobs Å	dcal Å
220	3.56	3.57
311	3.04	3.04
222	2.91	2.91
400	2.62	2.63
422	2.07	2.06
440	1.78	1.78
531	1.71	1.70
620	1.58	1.59
533	1.54	1.55
622	1.52	1.52

Table 2.4 MILLER INDICES AND hkl PLANES FOR $Y_2Sn_2O_7$

Plane hkl	dobs Å	dcal Å
220	3.58	3.58
311	3.05	3.05
222	2.92	2.92
400	2.53	2.53
331	2.32	2.32
422	2.07	2.07
511/333	1.95	1.95
440	1.76	1.79
620	1.59	1.60
533	1.54	1.54
511/711	1.43	1.42
642	1.40	1.40

Table 2.5 MILLER INDICES AND hkl PLANES FOR $Sm_2Ti_2O_7$

Plane hkl	dobs Å	dcal Å
220	3.61	3.61
311	3.07	3.07
222	2.94	2.94
400	2.54	2.54
331	2.33	2.33
511/333	1.96	1.96
440	1.80	1.80
531	1.71	1.72
620	1.61	1.61
622	1.53	1.53

Table 2.6 MILLER INDICES AND hkl PLANES FOR $Sm_2Sn_2O_7$

Plane hkl	dobs Å	dcal Å
220	3.68	3.67
311	3.13	3.13
222	2.99	2.99
400	2.59	2.59
331	2.38	2.38
422	2.12	2.12
511/333	1.99	1.99
440	1.84	1.83
531	1.76	1.75
620	1.63	1.64
622	1.56	1.56

the lattice parameter between a= 10.0 to 10.40 A^0 The reported planes for cubic spincel systems are[220] , [311] , [222], [400], [440], [531], [620] etc.

X-ray diffraction patterns of all the present pyrochlore samples were obtained by using monochromatic radiation at room temperature and are shown in Figs. 2.4 to 2.9 The lattice parameter 'a' is calculated by using least square method. The calculated and observed d values along with the planes for all the samples are given in Tables 2.1 to 2.6. The observed and calculated lathice spacing are very close to each other for all the observed planes.

The calculated lathice constants of $Y_2Ti_2O_7$ / $Sm_2Ti_2O_7$ agree with the reported values. (7,8). The values of lathice parameters for all the samples are given in Table 2.7. it is noted that lathice Constant increases with replacement of Ti by Sn and also Y by Sn and Ce. This is due to large ionic radii of respective elements. All the atoms in the pyrochlore unit cell occupies special positions with space group Fd3m. For $A_2B_2O_7$ these position are given by (9)

Ion	Location	Site Symmetry
16A	16d	$\bar{3}$ m (D_{3d})
16B	16c	$\bar{3}$ m (D_{3d})
48 O	48f	mm (C_{2v})
8 O'	8 b	$\bar{4}$3m (T_d)

Where origin is of B ion site.

From the pyrothlore structure the displcement of oxygens and the bond lengths can be calaulated by X-ray or neutron refinement structure analysis. The bond lengths are calculated by taking the ideal values of X = 0.3125 (5/16) for regular octahedra and u = 0.375 (3/8) for regular cube. The lathice parameters are generally ~ 10 A^0 whereas X parameter is found to range from 0.309 to 0.355 (with B - O ion chosen as origin). By using the following relations

$$B - o = a (u^2 - u + 9/32)^{1/2} \qquad \text{----------(2.5)}$$

$$A - o = a [(u+x -1/2)^2 + 2 (1/8 - x)^2]^{1/2} \qquad \text{----------(2.6)}$$

the bond lengths are calculated. The calculated bond lengths are given in Table 2.7

The density of the samples can be determined by measuring both the weight and volume of the samples, but it gives some error, so liquid immersion method have also been used to calculate the correct density of the sample. Hendrick and Jefferson (10) have dereloped a method to measure the density accurately. This method depends on immersing the solid in some liquid of known density in which the solid is completely insoluble. For this measurement liquid pyknometer was used. It was designed by Johnson and Adams (11) In the pyknometric method, the volume of the solid was more

accureately found by determining the changes in weight. The fundamental equation for the calculation of density ds of solid is

$$ds = \frac{W_s}{V_{DL}} \qquad \text{----------(2.7)}$$

Where V_{DL} is the volume corresponding to W_s grams of solid.

V_{DL} can be regarded as the amount of liquid (V_{DL} grams of density d_L), which would be displaced in grams of solid were put in to a completely liquid filled vessel.

The densities of present samples were determined by liquid immersion method described above. For this measurement tolune is used as a liquid. The meusured densites are shown in Table 2.8. The porosity of the samples was calulated by using the formula.

$$P = \frac{dx - ds}{dx} \times 100 \qquad \text{---------- (2.8)}$$

and $$dx = \frac{8m}{Na3} \qquad \text{----------(2.9)}$$

where ds is the actual density calculated by liquid immersion method,

M is molecular weight, a is the lathice constant and N is avogadro's number

The values of porosity and X- ray densities are listed in Table 2.9. It is observed that the porosity of these sampes are almost same and $\leq$ 17 %.

The average particle size for the present samples is also listed in Table 2.8 which is determined by using the relation.

$$t = \frac{0.9\lambda}{B\cos\theta.}$$

where B = half width maximum.

Table 2.7 Values of Lattice Constants and Bond lengths.

Sample	Lattice Constant Å	Bond lengths	
		A - O Å	B - O Å
$Y_2 Ti_2 O_7$	10.0981	3.275	2.184
$Ce_2 Ti_2 O_7$	10.3273	3.350	2.233
$Sm_2 Ti_2 O_7$	10.1933	3.306	2.204
$Y_2 Sn_2 O_7$	10.1422	3.290	2.193
$Ce_2 Sn_2 O_7$	10.3753	3.365	2.244
$Sm_2 Sn_2 O_7$	10.8060	3.369	2.246

Table 2.8 Values of X-ray density, Volume (actual) density and percentage porosity.

Sample	particle Size **t** nm	X-ray density **d x** gm/cc.	Actual density **d s** gm/cc	Porosity **p** %
$Y_2 Ti_2 O_7$	107.2	2.99	2.47	17.3
$Ce_2 Ti_2 O_7$	93.2	3.54	3.02	14.7
$Sm_2 Ti_2 O_7$	97.5	3.84	3.34	12.9
$Y_2 Sn_2 O_7$	104.6	4.04	3.73	7.3
$Ce_2 Sn_2 O_7$	78.6	4.50	3.73	17.1
$Sm_2 Sn_2 O_7$	98.4	4.64	4.02	12.5

REFERENCES

1. Swallow D. and Jordon A.K.;

   Proc. British Ceram. Soc. **2** ,1 (1964)

2. Sato T; ITEE Trans. Mag. Mater **6** ,795 (1970)

3. Nabarrow F.R.N.; Rept. Conf. Strength of Solids

   Phys Soc. London 75 (1948)

4. Herring C; J.Appl. Phys. **21** , 437 (1950)

5. Burke J.E.; "Kinetics of High temperature Processes"

   Edi W.D. Kingery N.Y. 109 (1959)

6. Zener C, Smith C.S.; Trans. AIME **175** , 15(1948)

7. Catherine H., Bernhardt J.W. and Judith K.S.;

   J.Solid st. Chem. **117**, 108 (1995)

8. L.H. Brixner; J., Inorg Chem. **3** , 7 1066 (1964)

9. M.A. Subramanian, G.Aravamudan and G.V. Subba Rao;

   Prog, Soild st. Chem. **15** , 58 (1983)

10. Hendricks S.B. and Jefferson M.E.; J. Opti. Soc. Am. **23** , 299 (1933)

11. Johnson and Adams L.H.;

    J. Am. Ceram. Soc. **34** , 563 (1912)